Photoelectron spectroscopy studies of growth, thermal stability, and alloying for transition metal-tungsten (111) bimetallic systems

J. J. Kolodziej* and T. E. Madey†
The Department of Physics and Astronomy and Laboratory for Surface Modification, Rutgers, The State University of New Jersey, Piscataway, New Jersey 08854-8019

J. W. Keister and J. E. Rowe
Physics Department, North Carolina State University, Raleigh, North Carolina 27695
(Received 22 February 2001; published 28 January 2002)

High-resolution soft-x-ray photoelectron spectroscopy using synchrotron radiation is used to study late-transition-metal films (Pt, Pd, Ir, Rh) on W(111). It is found that the films grow in a layer mode at 300 K. A single physical monolayer (ML) of each of these metals ''floats'' on the tungsten substrate and, upon annealing to $T>700$ K, the metal film-coated W(111) becomes faceted, i.e., covered with three-sided pyramids exposing {211} planes. During growth of Pt, Ir, and Rh films, at 300 K, for coverages exceeding 1 ML, atomic mixing at the interface is observed, driven by energy released in the adsorption process. Multilayer films of these metals on W(111), upon annealing, undergo complex transformations which include alloying, segregation, cluster formation, and faceting of the surface between clusters. It is demonstrated that despite the unusual complexity of the problem, soft-x-ray photoelectron spectroscopy allows for successful investigation of these transformations.

DOI: 10.1103/PhysRevB.65.075413 PACS number(s): 68.55.−a, 68.60.Dv, 64.75.+g, 81.05.Bx

I. INTRODUCTION

High-resolution core-level photoemission spectroscopy is extremely useful in studies of complex bimetallic systems for which, during formation, many concurrent phenomena such as alloying, surface segregation, cluster formation, or surface reconstruction may occur. Despite many challenges with data interpretation, high-resolution soft-x-ray photoelectron spectroscopy (SXPS) is a very useful technique for studies of bimetallic interfaces since it provides identification of the surroundings of various atoms via measurements of core-level shifts.

Transition metals, their alloys, and thin films have attracted much attention recently, both because they have interesting physical properties, and because of the variety of their technological applications as catalysts, shape memory alloys, and in new magnetic materials. As shown recently, the atomically rough tungsten (111) surface covered with films of certain metals (Pt, Pd, Rh, Ir, Au) and annealed to temperatures 700–800 K undergoes massive reconstruction to form three-sided pyramids of nanometer scale dimensions with {211} planes as facet sides.[1,2] This evidence for instability of surface morphology in a bimetallic system has important implications: effective control over growth and morphology of nanostructure features on surfaces is essential for the design and operation of future generations of devices.

In previous studies we have reported on growth and alloying of late-transition-metal films on the tungsten (211) surface.[3,4] In the present work we focus on the growth and thermally activated restructuring (faceting) induced by late-transition-metal films on atomically rough tungsten (111). It is demonstrated that the extremely complex structures present on these bimetallic surfaces may be successfully resolved and investigated with the SXPS technique.

Specifically, in the present study, we report high-resolution $4f_{7/2}$ photoemission spectra from $5d$- and $4d$-late-transition-metal (Pt, Pd, Ir, Rh) covered tungsten surfaces as a function of coverage and annealing temperature. Where possible (Pt and Ir on W), admetal $4f$ core-level spectra have been measured and correlated with the substrate spectra.

There are several interesting findings in these studies of metals on W(111). First, we report evidence for segregation of single monolayers of Pt, Pd, Ir, and Rh on the atomically rough W(111) surface upon annealing [in contrast to reports of surface alloys on planar W(100) under certain conditions; cf. Refs. 5 and 6]. Second, we find strong evidence for intermixing at the interface for multilayer deposition of several metals (Pt, Rh, Ir) on W(111) at room temperature. This is unexpected for the thin-film community; it has been generally believed that thin films of high-melting-T metals form abrupt interfaces.

The present results have implications beyond the specific systems studied. Rapidly developing highly accurate first-principles theoretical methods for solid-state energetics allow now for precise description of bulk and surface properties of materials (cf. Refs. 7–10). For example, a comprehensive table of segregation energies for transition-metal impurity monolayers on close-packed surfaces of transition metals has been published recently.[11] We believe the time is ripe for careful examination of phenomena occurring at interfaces and surfaces of bimetallic systems with highly surface-sensitive techniques, in order to test and to stimulate further theoretical work.

This paper is organized as follows. After the description of experimental procedures we present results and data analysis for four different metallic overlayers (Pt, Pd, Ir, Rh) on W(111); all of these metals are known to induce faceting of W(111) to {211}. The Pt/W(111) data are described in greatest detail to illustrate the analysis and curve-fitting pro-

cedures. The essential features of the remaining three overlayers are presented more briefly. Finally all of the data are discussed to analyze the film growth, thermal stability, segregation, and alloy formation. The findings for W(111)-based bimetallic systems (similarities as well as strong differences) are compared with the earlier study of W(211)-based systems.

II. EXPERIMENTAL METHODS

The experiments have been performed in a stainless-steel ultrahigh-vacuum experimental system at the National Synchrotron Light Source of Brookhaven National Laboratory, on beamline U4A. Details of the experimental setup are described elsewhere.[12] The total spectral resolution is ~ 0.2 eV at 150 eV and below 0.1 eV at 80 eV photon energy. Typically the x-ray beam and the energy spectrometer axis form an angle of 45° and the x-ray beam is incident at 45° onto the sample. The photon flux is monitored and the measured spectra are normalized to account for the slowly changing photon flux. The tungsten (111) substrate is prepared by repetitive heating in oxygen (1×10^{-7} Torr) at 1300 K, followed by an abrupt increase of substrate temperature to 2300 K for a few seconds (flash). The experimental setup contains several metal dosers used for deposition of platinum, palladium, rhodium, iridium, and gold. Special care is taken to outgas the dosers before their use. Dosers are shielded during operation by cooled surfaces and the background pressure during operation does not exceed 2×10^{-10} Torr. Details of the coverage calibration have been described in Refs. 3 and 4. Sample temperature is measured by a W5%Re–W26%Re thermocouple spot-welded to the side of the W crystal.

In order to investigate thermally activated processes occurring on overlayer films and at the interface, stepwise annealing to increasingly higher temperatures is used: after metal deposition the sample is annealed in a sequence of increasing temperatures ranging from 400 to 2300 K. After each step the sample is cooled, and SXPS data are recorded.

III. RESULTS AND DATA ANALYSIS

A. Platinum

1. Film growth

In Fig. 1, a sequence of SXPS spectra associated with the growth of a Pt film on the W(111) surface is shown. The Pt $4f_{7/2}$ peak shape is distinctly different for coverages of 1/3, 2/3, and 1 ML [where one physical monolayer (ML) is defined as the coverage needed to shadow all substrate atoms: $\sim 1.7\times10^{15}/\mathrm{cm}^2$]. This is a simple consequence of the structure of a single pseudomorphic monolayer on bcc (111) and a layer-by-layer film growth. The pseudomorphic layer on a bcc (111) crystal surface contains three geometrical ''layers'' containing atoms in different chemical configurations.[13] A complete adlayer (1 ML) contains equal numbers of atoms of all three types. We have performed a decomposition of Pt peaks using as model functions Doniach-Sunjic (DS) line shapes. The $4f_{7/2}$ feature, as demonstrated in Fig. 2, is single-component at 1/3 ML, double-component at 2/3 ML,

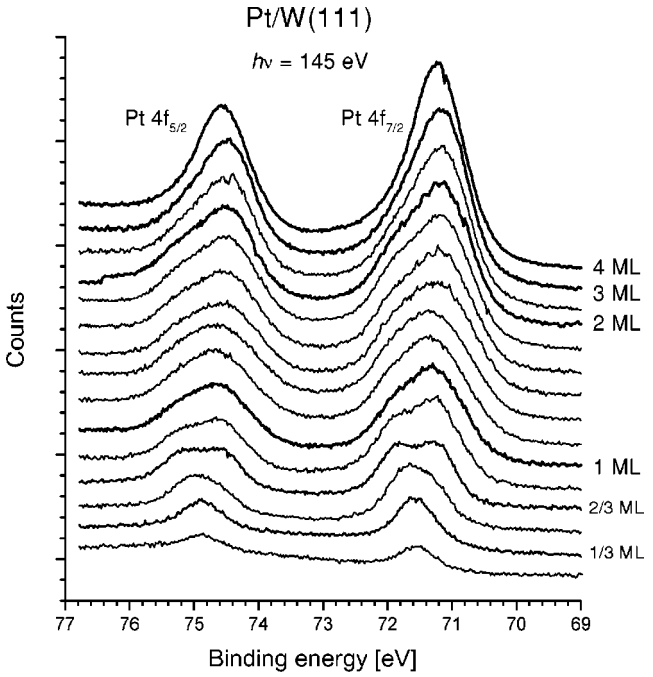

FIG. 1. The Pt $4f$ spectral region recorded during growth of Pt films on W(111) at 300 K.

and triple-component at 1 ML. All components have comparable intensity. Such an evolution of the Pt SXPS peak evidences a layer-by-layer character of growth (in the sense of geometrical ''layers''). For higher (multilayer) coverages the Pt $4f_{7/2}$ feature is smooth and shapeless. This is very different from the case of a pseudomorphic film on W(211) (Ref. 4) where the single DS lines could be associated with physical layers at the interface and at the surface. In contrast, for a Pt film on W(111), there are differences in positions of SXPS lines associated with different geometrical layers within the same physical layer at the interface and at the surface. Thus the $4f_{7/2}$ SXPS feature for a Pt pseudomorphic film on W(111) is composed of slightly shifted multiple components and unique decomposition of the $4f$ feature is not possible. This is illustrated in Fig. 2(d) where a very accurate Doniach-Sunjic lines fit produces an unphysical surface-to-bulk components ratio (approximately 1:1 is expected based on photoelectron attenuation length). As illustrated in the inset in Fig. 3, the dependence of the substrate W $4f$ peak intensity on the film thickness is exponential. Since one dose corresponds to approximately 1-ML coverage it is difficult to judge whether the growth is a true layer-by-layer or random (''sticks-where-it-hits'') growth mode. On the other hand the low-energy electron-diffraction (LEED) image remains 1×1 during growth but spot sharpness deteriorates with increasing coverage. These observations indicate that the Pt deposit uniformly covers the W substrate, however, the surface of the film is not atomically flat. [In order to illustrate the difference in attenuation of substrate signal for the flat and the 3d growth mode we included an attenuation curve for Fe on W(111) growth, see the inset in Fig. 3. The Fe on W attenuation is characteristic of $3d$ growth above 2-ML (two doses) coverage. The Pt on W attenuation is characteristic of flat growth.]

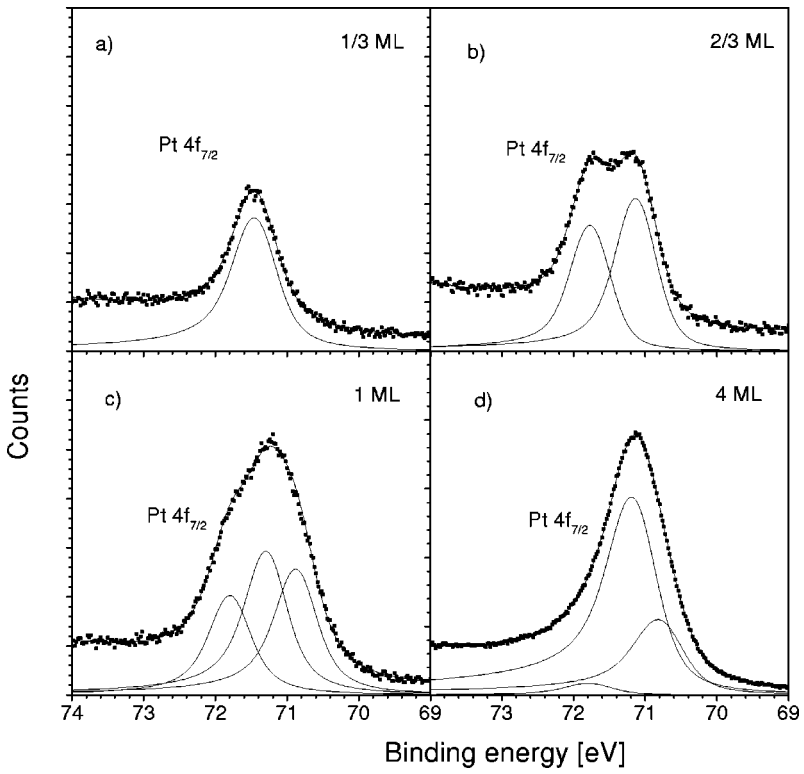

FIG. 2. Doniach-Sunjic (DS) Pt $4f_{7/2}$ lineshape fits for a few different thicknesses of a Pt film on W(111): (a) for 1/3-ML, (b) for 2/3-ML, (c) for 1-ML, and (d) for 4-ML coverage.

A very interesting property of the Pt/W(111) system observed during growth of a Pt film at room temperature is that satellite peaks appear in the W $4f$ region after single-monolayer coverage is exceeded. These peaks are shifted by ~ 1 eV to higher binding energy, relative to W $4f$ bulk peaks (see Fig. 3). These peaks have been previously assigned to a tungsten impurity in the Pt host (or a dilute W alloy)[4] and their presence during adsorption of Pt on W(111) provides evidence that mixing at the Pt/W interface occurs as a result of the adsorption process. It can be seen that for lower coverages (2–3 ML) the satellite W $4f_{7/2}$ peak is slightly shifted relative to the dilute W in the Pt $4f_{7/2}$ peak (the Pt film is too thin and the strict ''dilute'' situation is not possible). Above 3-ML coverage the additional peak appears at the exact position of the ''dilute alloy'' peak which is shifted by 0.95 eV with reference to the bulk W position (Ref. 4). The intensity of the dilute alloy peak relative to the intensity of the substrate peak increases until a coverage of 6 ML is reached. This indicates that the mixing at the interface continues up to 6-ML coverage.

2. Annealing of Pt films

The thermal evolution of the W(111) surface covered with 1 ML of Pt has been monitored by LEED and SXPS (see Fig. 4). Each SXPS spectrum shown in Fig. 4 is labeled with the corresponding type of surface reconstruction as determined by LEED. As-dosed Pt $4f$ peaks display shoulders on the high binding-energy side, resulting from their multicomponent character as discussed above. Below 500 K the film maintains 1×1 structure. Above 500 K the Pt SXPS peaks lose their distinct shoulders and LEED indicates a $(2\sqrt{3}\times2\sqrt{3})R30°$ reconstructed surface. This configuration is

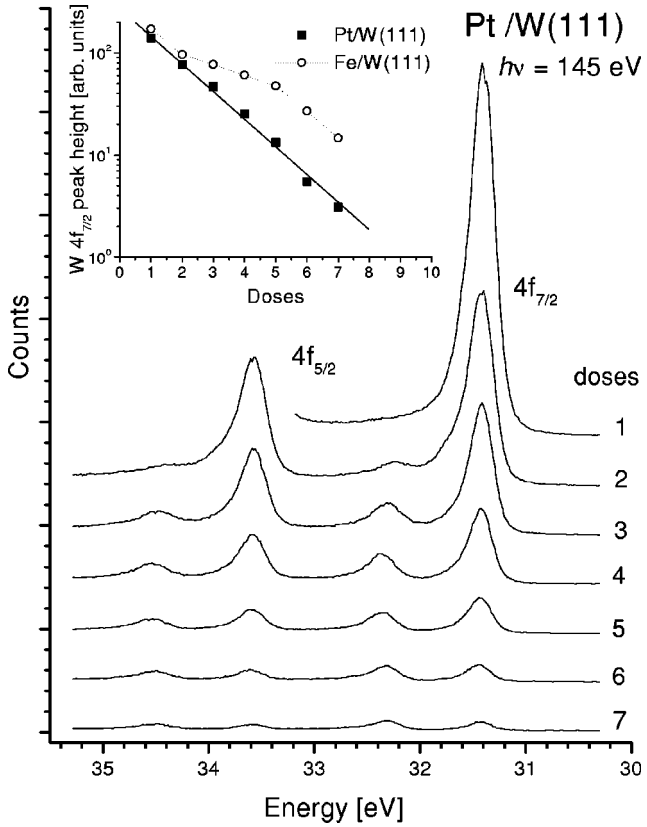

FIG. 3. W $4f$ spectra associated with growth of a multilayer Pt film on W(111) at room temperature. The inset shows the height of the W $4f_{7/2}$ peak as a function of coverage. One dose corresponds to ~ 1 ML (solid line, square points). For comparison we show the attenuation curve for a case when the flat growth mode breaks down at ~ 2-ML coverage [case of Fe/W(211): dotted line, circle points].

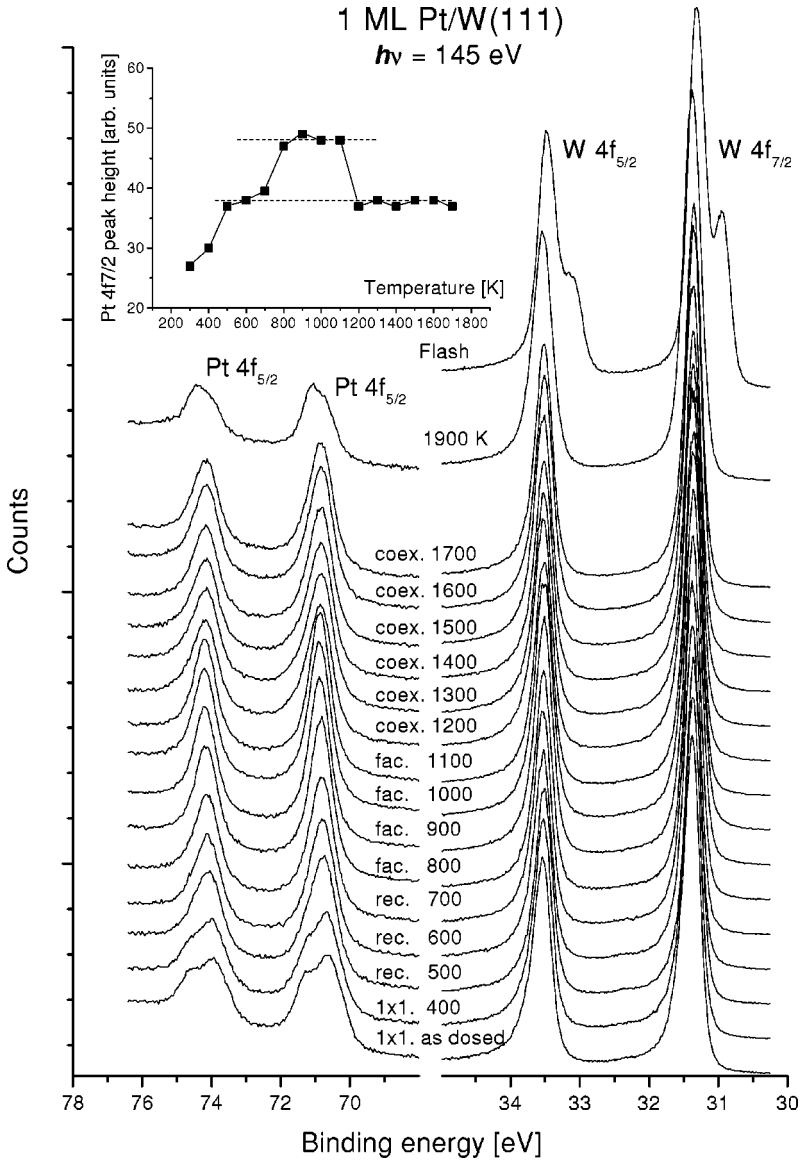

FIG. 4. Annealing sequence for a 1-ML Pt film on W(111). The Pt 4*f* and W 4*f* spectral regions are shown following annealing to the indicated temperature for 1 min. The meanings of reconstruction labels are the following: ''rec.,'' $(2\sqrt{3}\times 2\sqrt{3})R30°$, ''fac.,'' faceted, and ''coex,'' coexistence of faceted and ''rec.'' The inset shows a Pt $4f_{7/2}$ peak height as a function of annealing temperature.

stable up to a temperature of ~700 K where the faceting surface phase transition occurs. The faceting transition can be identified both by a change in the LEED pattern (see Refs. 14 and 15 for a description of the ''faceted'' LEED pattern) and by narrowing of the Pt 4*f* feature, which is an effect of a change in the Pt peak characteristic of a planar Pt adlayer on W(111) (multicomponent) to that characteristic of a Pt adlayer on W(211) (single component). (Facets are 10–100 nm in size and their edges make little contribution to the SXPS peak intensity.) This is visualized in Fig. 4 (inset) which shows the height of the Pt $4f_{7/2}$ peak as a function of annealing temperature. The narrowing of the Pt feature results in increased height of the feature. The plateau between 700 and 1100 K is correlated with the faceted LEED pattern. Above 1100 K the Pt $4f_{7/2}$ peak height decreases and the LEED pattern becomes mixed [faceted and $(2\sqrt{3}\times 2\sqrt{3})R30°$] suggesting the coexistence of faceted and planar regions on the surface. In the W $4f_{7/2}$ region no changes in the peak shape and intensity are seen throughout the whole annealing temperature range. Above the thermal-desorption threshold for Pt, W 4*f* features associated with surface tungsten atoms appear (see also Refs. 16 and 17).

In Fig. 5, Pt 4*f* and W 4*f* spectra associated with annealing of a 5-ML thick Pt film on W(111) are shown. For temperatures below 1000 K the observed peak changes resemble those observed during annealing of the Pt/W(211) system.[4] Peaks in the W 4*f* region do not change [see the W $4f_{7/2}$ dilute alloy peak formed upon Pt adsorption at the 32.35-eV binding energy (BE) and the substrate peak at 31.4 eV] up to an annealing temperature of 600 K. Above this temperature the dilute alloy peak increases in intensity and above 800 K it shifts towards the substrate peak, evidencing formation of a saturated alloy. In the dilute alloy phase Pt 4*f* peaks appear unchanging (since the number of Pt atoms in contact with W atoms is low), but the alloy saturation is accompanied by shifts of Pt features to higher binding energy, and by splitting into two separate components (at ~72.4-eV BE which we attribute to the Pt in the Pt/W alloy and at 71.5-eV BE attributed to the Pt segregated to the alloy surface). Above 1000 K there is a significant increase in the intensity

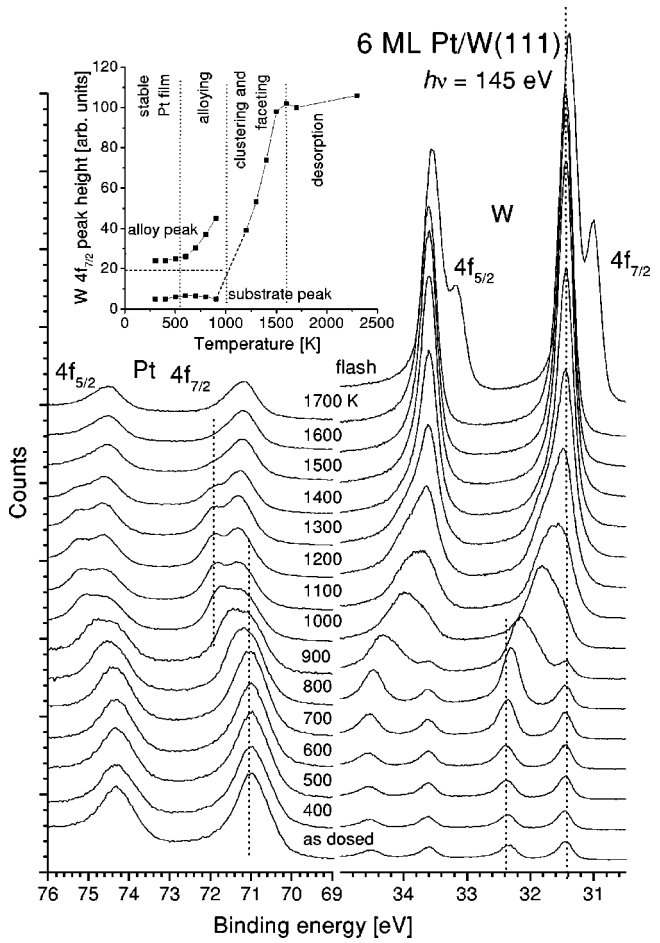

FIG. 5. Pt $4f$ and W $4f$ SXPS spectra associated with the annealing sequence for a 6-ML Pt film on W(111). Annealing time is 1 min. The inset shows the intensity of substrate and dilute alloy W $4f_{7/2}$ peaks as a function of temperature.

of the W $4f_{7/2}$ substrate peak and a decrease in the intensity of the Pt $4f_{7/2}$ alloy peak at 72.4-eV BE. This peak becomes invisible at 1500 K, i.e., $\sim$200 K below the threshold temperature for thermal desorption of Pt from the Pt-W alloy.[18] These observations indicate that upon annealing to $T > 1100$ K the alloy film evolves into three-dimensional clusters whose areas exposed to the SXPS probe are insignificant. The substrate surface between the clusters remains covered with a 1-ML Pt film as evidenced by the intensity and position of the surface Pt feature and the lack of W surface peaks at temperatures 1400–1700 K. The inset in Fig. 5 shows the intensity of W $4f$ features versus annealing temperature. The different phases of thermal evolution of the Pt/W(111) denoted on this graph have been assigned according to the above considerations.

B. Palladium

Due to the limited photon energy range of our apparatus (30–200 eV), the data for Pd/W could be obtained only in the $4f_{7/2}$ region of tungsten (the $3d$ levels of Pd are beyond the accessible photon energy range). A set of SXPS W $4f$ spectra for 1-ML Pd on W(111) recorded following annealing to increasingly higher temperatures is shown in Fig. 6. A shift of the W $4f_{7/2}$ peak corresponding to the faceting transition is visible at 800 K. The W surface peaks appear when the sample is annealed to temperatures at which Pd desorption from the Pd/W surface becomes efficient ($T > 1300$ K). The W $4f$ peak shift due to faceting is caused by a change of the Pd/W interface and Pd pseudomorphic film from (111) to (211) as illustrated in Figs. 7(a)–7(c). Annealing of the 1-ML film on W(211) does not cause a change in the W peak shape—the Pd/W(211) system does not undergo transformations upon annealing below Pd desorption temperatures [Fig. 7(a)]. The faceted Pd/W(111) and Pd/W(211) SXPS features are in fact identical, within experimental uncertainty, see Fig. 7(b). (The facet edges occupy little surface area and do not influence the SXPS spectra.) A direct comparison of the W $4f_{7/2}$ peaks for the planar and faceted Pd-covered W(111) surface is shown in Fig. 7(c). A more detailed analysis of W $4f$ peak shifts upon faceting can be found in Ref. 17.

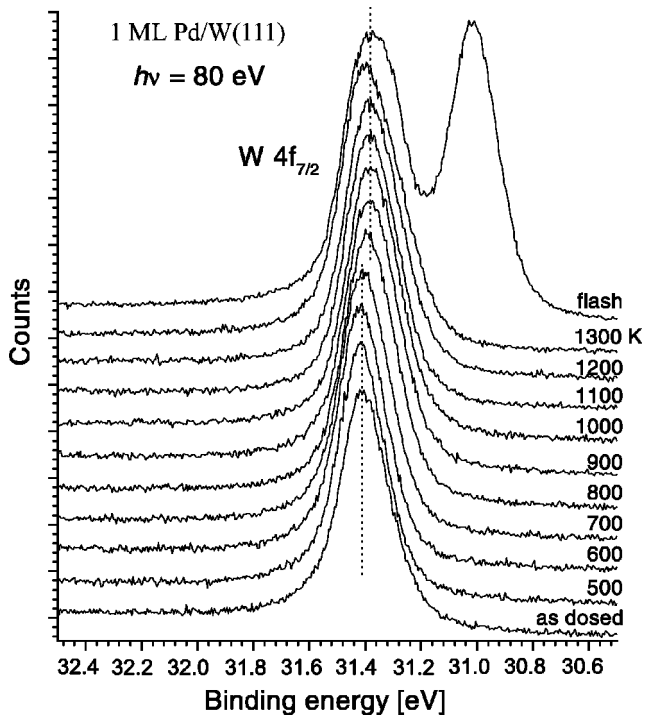

FIG. 6. W $4f_{7/2}$ SXPS spectra associated with annealing of a 1-ML Pd film on W(111).

Figure 8 shows W $4f$ peaks during growth of a multilayer Pd film on W(111). The dependence of the substrate peak height on Pd coverage is exponential (see inset in Fig. 8) indicating a flat form of growth. In contrast to Pt on W(111) (see Sec. III A 2 above), for Pd deposited on W(111) no satellite peaks have been observed in the W $4f$ region indicating no evidence of intermixing of Pd/W upon deposition.

For 10-ML coverage of Pd the W $4f$ substrate peaks are attenuated and scarcely visible (see in Fig. 9 the two lowest spectra in the sequence). Upon annealing, the film of Pd on W(111) undergoes complex changes. At annealing temperatures 450–500 K the substrate peaks increase in intensity, indicating that the layer is corrugated and the substrate areas

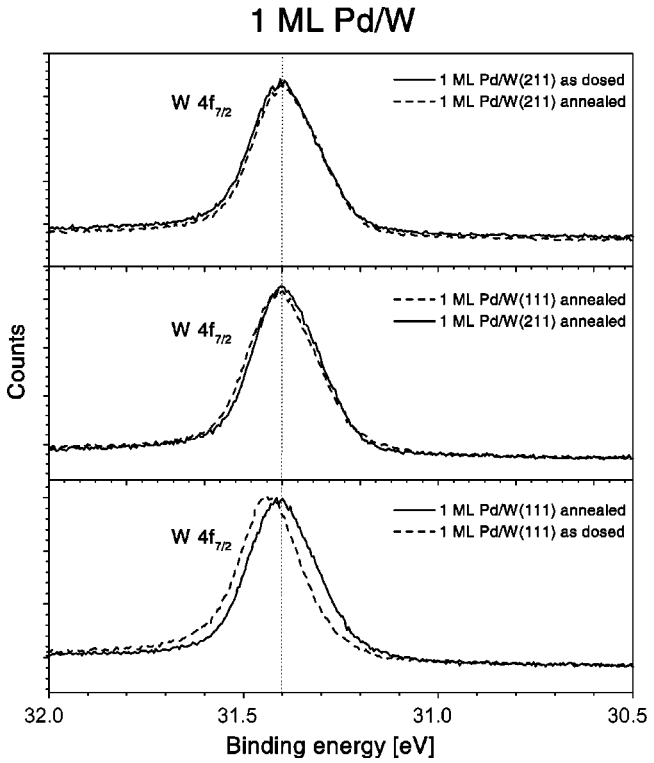

FIG. 7. A comparison of W $4f_{7/2}$ peaks for 1-ML Pd-covered W(211) and W(111).

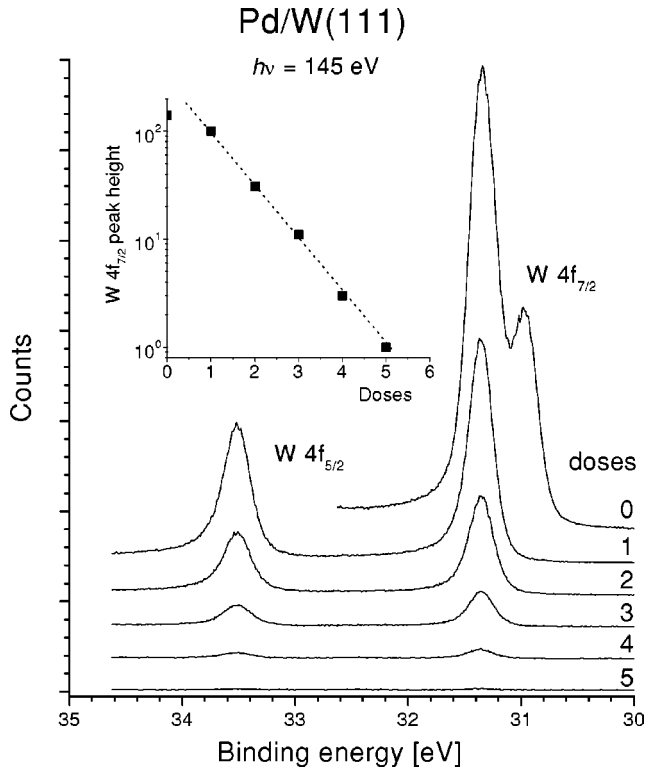

FIG. 8. W $4f$ spectra associated with growth of a multilayer Pd film on W(111) at room temperature. The inset shows the height of the W $4f_{7/2}$ peak as a function of coverage; one dose corresponds to ~1 ML.

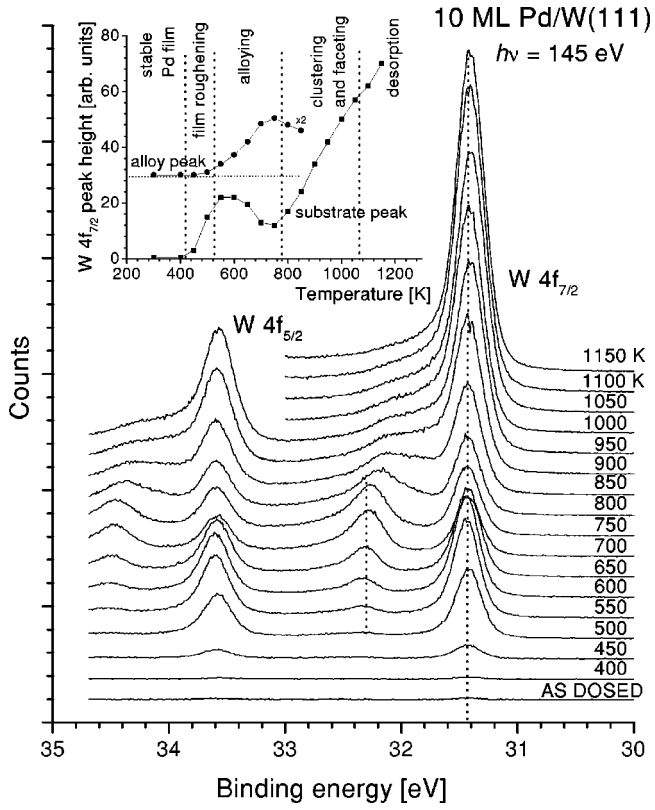

FIG. 9. W $4f_{7/2}$ SXPS spectra associated with annealing of a 10-ML Pd film on W(111). The inset shows the height of W $4f_{7/2}$ peaks as a function of annealing temperature.

covered with a thinner film are exposed. The dilute alloy peak appears at 550 K and increases up to 750 K. Simultaneously the substrate peak intensity is reduced back, reflecting increased attenuation of the W $4f$ peak by a corrugated alloy film (this may be an effect of the increasing alloy film volume due to incorporation of tungsten atoms into the film). Above 750 K the saturation of the alloy (evidenced by broadening of the alloy W $4f$ features) is accompanied by another substantial increase in the substrate peak intensity. At ~950 K, the intensity of the alloy peak decreases, evidencing the formation of relatively large three-dimensional clusters with small effective areas seen by x-ray photoelectron spectroscopy (XPS). [The threshold for thermal desorption of Pd from the Pd-W alloy formed by annealing is 1200 K (Ref. 2).] The W surface between clusters is covered with a 1-ML Pd film (no W $4f$ surface features are visible) and is faceted, as evidenced by the SXPS W peak position. The intensity of the substrate W $4f$ features vs annealing temperature is plotted in the inset in Fig. 9. The evolution phases of the Pd/W(111) system are denoted on this graph.

C. Iridium

The $4f$ SXPS spectra associated with the growth of multilayer Ir on W(111) are shown in Figs. 10 and 11. Previously it has been found for Ir/W(211) that Ir SXPS $4f$ peaks are not shifted if the Ir neighbor atom is exchanged by a W atom.[4] Such stability of the Ir atom electronic structure

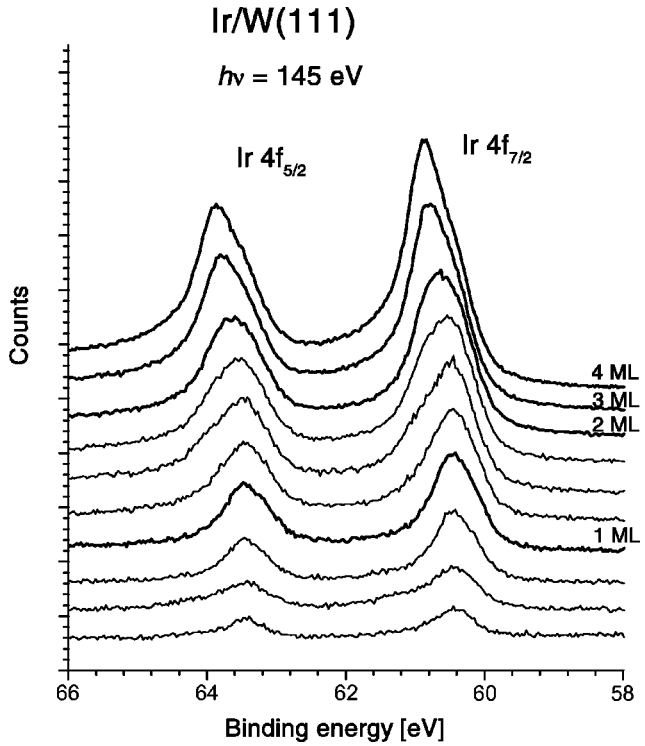

FIG. 10. An Ir $4f$ spectral region recorded during growth of an Ir film on W(111) at 300 K.

is also evident for the Ir/W(111) system, see Fig. 10, where in contrast to Pt/W(111), there is little variation of the Ir peak shape in the submonolayer coverage regime. The feature is clearly multicomponent but the different lines are due to atoms with different coordination numbers rather than due to atoms at the interface experiencing different chemical interactions with the substrate (which was the case for Pt/W). At 4 ML the ''surface'' shoulder on the low BE side is much less intense than for Ir/W(211) indicating that it may be associated with the top geometrical layer rather than with a top physical layer [which was the case for W(211)-based systems].

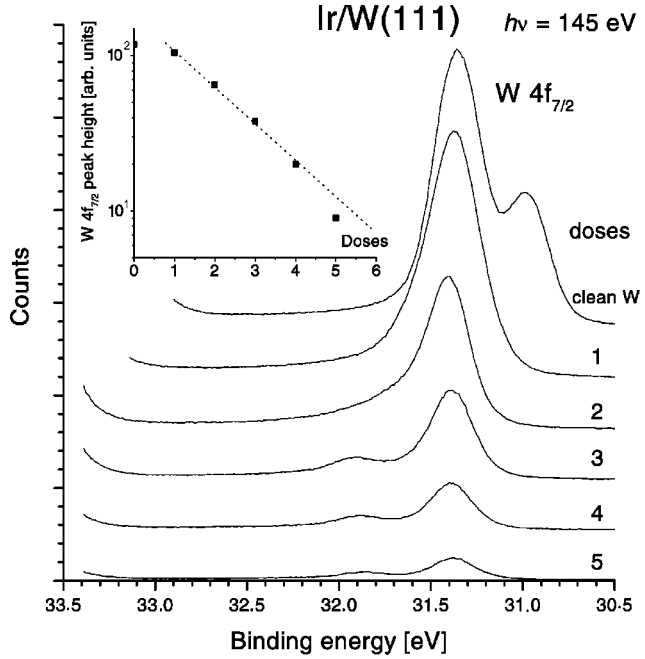

FIG. 11. W $4f$ spectra associated with growth of a multilayer Ir film on W(111) at room temperature. The inset shows the height of the W $4f_{7/2}$ peak as a function of coverage; one dose corresponds to ~1-ML coverage.

The dependence of the substrate XPS peak intensity on the film thickness is exponential, see the inset in Fig. 11. This indicates that the growth proceeds in a flat mode. (The small deviation of experimental data from the straight line in Fig. 11 is assigned to increase in deposition rate arising from gradual thinning of the Ir wire which is the source of Ir atoms.) For coverages greater than 2 ML additional peaks appear in the W $4f$ region evidencing an interface mixing similar to the one observed for Pt/W(111) (Sec. III A). These peaks are shifted by 0.5 eV to higher BE, and we assign these peaks to a W impurity in an Ir host (or dilute W in an Ir alloy, cf. Ref. 4).

The annealing sequence for 1 ML of Ir/W(111) is presented in Fig. 12. At different phases of annealing the W $4f$ spectra show rather complex behavior. As shown by LEED the ''as-dosed'' film surface has a $(2\sqrt{3}\times 2\sqrt{3})R30°$ structure and the SXPS Ir $4f_{7/2}$ feature displays a shoulder on the high binding-energy side of the SXPS peak. Upon heating to 500 K the LEED pattern changes to $(\sqrt{3}\times\sqrt{3})R30°$ and a shoulder appears on the high BE side of the W $4f$ feature. Above 800 K the W $4f_{7/2}$ peak becomes single-component and the LEED pattern changes indicating a faceting of the Ir film covered surface to (211). Upon further heating LEED shows coexistence of faceted and $(\sqrt{3}\times\sqrt{3})R30°$ reconstructed regions. The shoulder on the high BE side of the Ir peak reappears and the $4f$ feature resembles closely that before the faceting transition. These observations indicate that the surface has been converted partially to a planar one. Above 2100 K the monolayer desorption threshold is reached and the surface W $4f$ components are finally seen on the low BE side (Fig. 12).

In Fig. 13 an annealing sequence for ~7 ML of Ir on W(111) is shown. Dilute alloy peaks are present in the W $4f$ region for annealing temperatures up to 1000 K. Within this temperature range Ir $4f$ peaks show little variation. Above 1100 K the W $4f$ alloy peaks shift to lower BE and broaden indicating the formation of a saturated alloy film. At 1000 K the Ir $4f$ features change; the bulk Ir peak decreases in height, which reflects the decreased content of Ir in the bulk of the film. Within the range 1300–1700 K the system does not undergo further transformations as evidenced by constant SXPS shapes and intensities. This is illustrated in the inset in Fig. 13. Around 2000 K the Ir bulk alloy $4f$ components disappear as a result of thermal desorption of the Ir-W alloy.

D. Rhodium

For rhodium (a $3d$ metal), the data are limited to the $4f$ levels of the W substrate. During the growth of Rh films on W(111) the attenuation of substrate W $4f$ features is exponential as a function of coverage, evidencing a flat form of

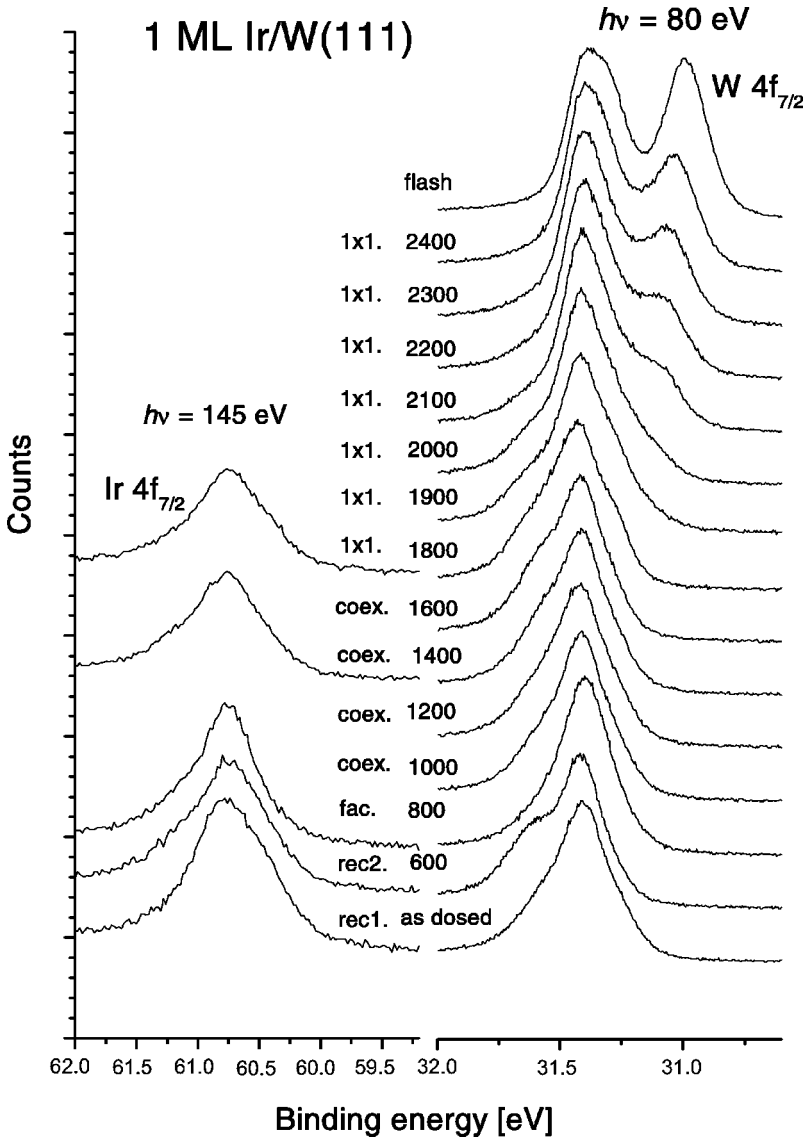

FIG. 12. Ir $4f_{7/2}$ and W $4f_{7/2}$ SXPS spectra associated with the annealing sequence for a 1-ML Ir film on W(211). Annealing time is 1 min. The meanings of the reconstruction labels are the following: "rec1.," $(2\sqrt{3}\times 2\sqrt{3})R30°$, "rec2.," $(\sqrt{3}\times\sqrt{3})R30°$, "fac.," faceted, and "coex.," coexistence of faceted and "rec2."

growth of Rh on W(111), see the inset in Fig. 14. For coverages higher than 1 ML additional peaks characteristic of a Rh impurity in the W host appear (see Fig. 14) shifted by ~ 0.5 eV to higher BE indicating adsorption-triggered interface mixing similar to that observed for Pt and Ir/W(111) (discussed in Secs. III A and III C).

An annealing sequence for ~ 8 ML of Rh on W(111) is shown in Fig. 15. The as-dosed spectrum show peaks due to the attenuated W substrate and dilute W in Rh. Above 500 K the two peaks increase concurrently. Above 650 K the dilute alloy Rh peak increases further while the substrate peak decreases, similar to Pd/W(111) (Sec. III B). The dilute Rh-W phase exists below an annealing temperature of 850 K. At 900 K the alloy peak broadens and shifts to lower binding energy. Simultaneously the substrate peak increases its intensity. Above 1000 K the alloy-related feature is almost invisible suggesting that the alloy forms large three-dimensional clusters. Around 2000 K the W surface peaks appear as a result of thermal desorption of Rh from the surface.

IV. DISCUSSION

A. Single monolayer films on W(111)

In general the deposition of metal on metal at room temperature leads to a metastable configuration. This configuration reflects the kinetics of deposition, diffusion, and growth processes, and the existence of diffusion (reaction) barriers.[7] This metastable state can survive in a limited temperature range. Annealing causes the energetic barriers to be overcome and the system lowers its free energy through intermixing and modification of the surface structure. Finally if the annealing temperature/time is sufficient the system may approach the global energy minimum.

Bimetallics involving transition metals are often extremely complex and synchrotron-radiation-based soft-x-ray photoelectron spectroscopy is a technique of choice for studying these systems. However, recent advances in accurate first-principles computational techniques have made it possible to calculate reliable segregation energies for a large number of close-packed transition-metal alloy surfaces.[11]

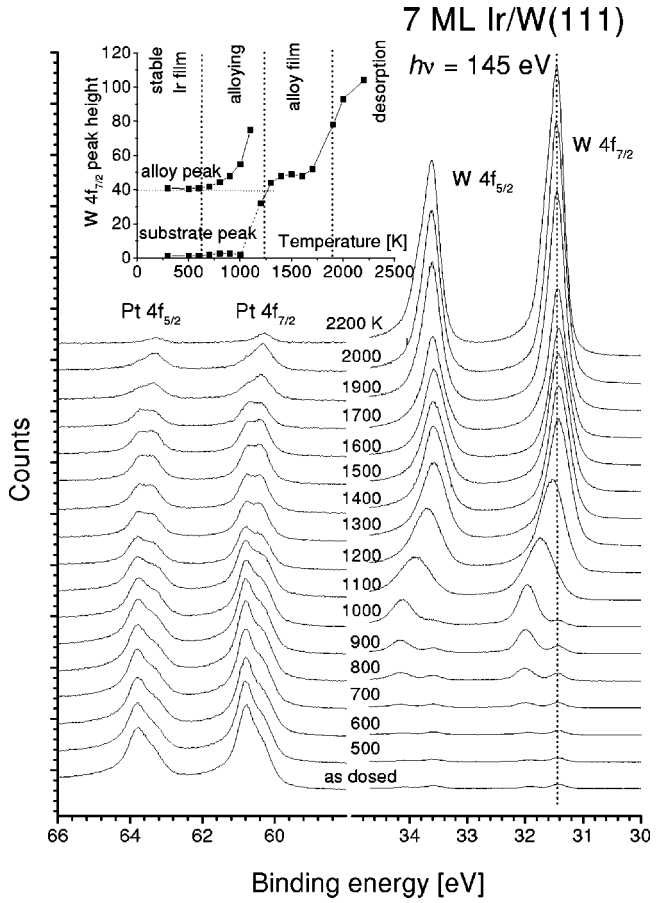

FIG. 13. Ir $4f$ and W $4f$ SXPS spectra associated with the annealing sequence for a 7-ML Ir film on W(111). Annealing time is 1 min.

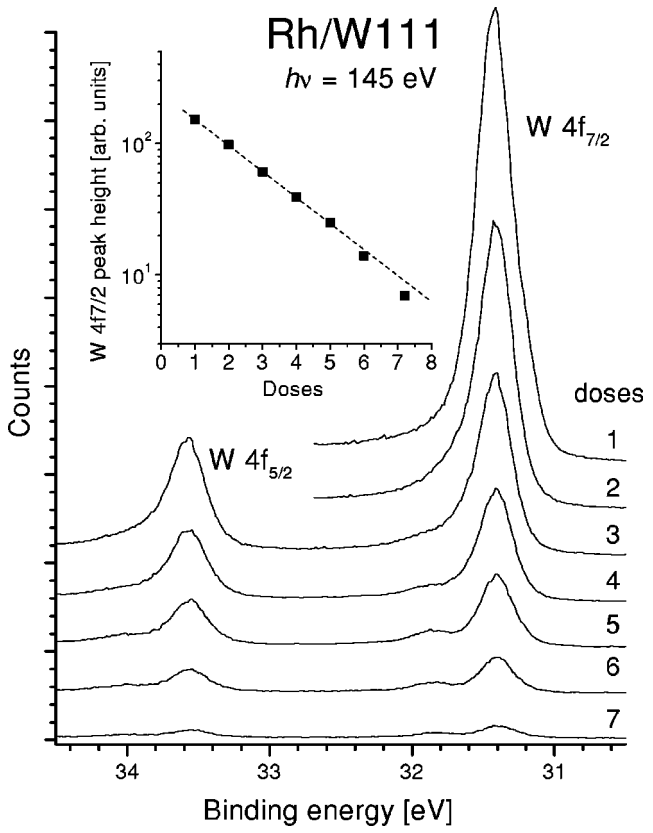

FIG. 14. W $4f$ spectra associated with the growth of a multilayer Rh film on W(111) at room temperature. Inset shows the height of the W $4f_{7/2}$ peak as a function of coverage; one dose corresponds to ~ 1 ML.

Such complete data arrays are extremely helpful in understanding and analyzing experimental data.

During annealing, if the segregation energy is negative, a metastable film of metal on a metal substrate will eventually dissolve into the bulk. If the segregation energy is positive, the metal tends to stay in the surface layer. However, the entropy factor in the free energy always favors an intermixed system and due to this factor at temperatures high enough to overcome diffusion barriers, the deposit may be slowly lost into the bulk.

Segregation energies for transition metals on the close-packed (110) surface of W have been calculated by Ruban *et al.*[11] Although in extreme cases the surface segregation energy may reverse its sign depending on the crystal face (for example, the PtNi alloy[19]) usually it is reasonably well described by a bond breaking model, from which it is assessed that the segregation energies scale by a factor up to 1.7 going from close-packed to open surfaces.[20] Based on the calculation of Christensen *et al.*,[7] it is expected that all metals reported here strongly segregate from a W host on both (211) and (111) crystal faces. This is indeed seen in our experimental data; a single physical monolayer of deposited metal (Pt, Pd, Ir, Rh) tends to remains on top of W(111). These findings are also consistent with previous data obtained by low-energy ion scattering,[21] and Auger electron spectroscopy (AES).[14,15] Similar segregation phenomena have been seen on W(211) with our previous SXPS studies.[4] For 1-ML Ir on W(111) annealed to $T=600$ K the change in the LEED pattern and the additional shoulder in the W $4f$ spectrum indicate formation of an ordered surface alloy phase.

Planar W(111) covered with 1 ML of Pt, Pd, Ir, and Rh is unstable upon heating, and a massive reconstruction occurs if the surface is heated above 700 K. As a result the surface is covered with pyramidal facets exposing {211}-type planes.[1] Following this transformation a monolayer of deposited metal still ''floats'' on the substrate.

For W covered with a single-monolayer metal film its W $4f$ SXPS peaks are composed of bulk and interface components. As a result of the faceting reconstruction the interface is converted from a (111) to (211) type, and the interface component of the SXPS features changes. This change is most apparent for the Pd/W system; for other systems studied the change is small (see also Ref. 17). An effect of faceting is also visible in the changing shape of overlayer metal (Pt and Ir) $4f$ SXPS peaks; faceted surfaces which expose {211} planes covered by 1-ML films produce single-component $4f$ features, as opposed to planar (111) surfaces which produce $4f$ features that cannot be described by single DS line shapes.

As evidenced by LEED, ultrathin late-transition-metal films on W(111) grown at room temperature are pseudomor-

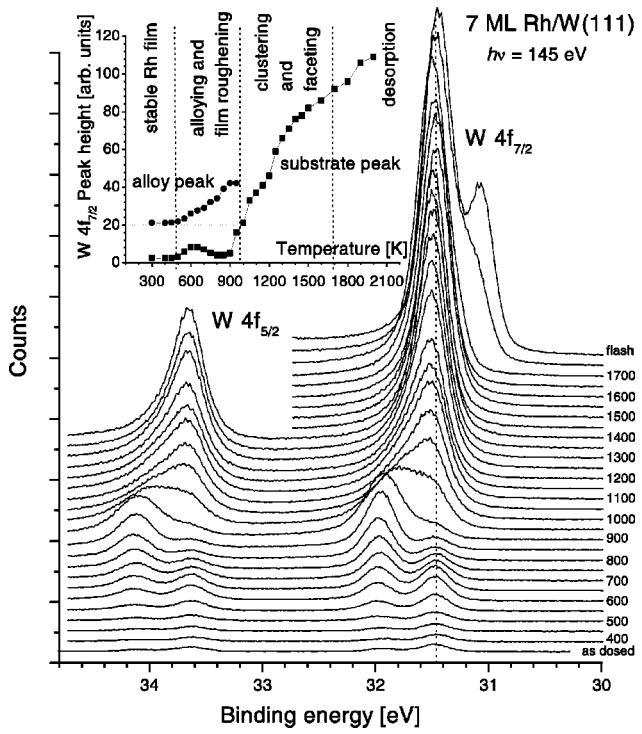

FIG. 15. W $4f_{7/2}$ SXPS spectra associated with the annealing sequence for a ~7-ML Rh film on W(111). Inset shows the substrate and dilute alloy W $4f_{7/2}$ peak intensity vs coverage.

phic. Results obtained for Pt/W(111) indicate that for coverages less than a single physical monolayer the growth has a well-defined layer-by-layer character. Distinct SXPS peaks for different geometrical ''monolayers'' in the pseudomorphic (111) bcc layer indicate that each lower layer is completed before the next one starts to grow. This is an important observation which helps in understanding the faceting surface phase transition. As shown in Ref. 22 the driving force for the transition is a surface energy difference between film covered W(111) and W(211) surfaces. The critical coverage for faceting to occur is 1 ML. Locally the coverage may reach 1 ML (in $2d$ islands) if the average coverage exceeds 2/3 ML. Such faceted 2d islands on a W(111) surface have been indeed revealed in recent LEEM and scanning tunneling microscopy (STM) studies.[23,24] In the present work the faceting transition has been observed on fully covered W(111) surfaces for annealing temperatures greater than 700 K for Pt, Pd, and Ir films. Interestingly the Pd-covered faceted surface is the most stable. Annealing the Pd-covered faceted W(111) surface causes an increase in the facet size but the overall character of the surface does not change. In contrast Pt- and Ir-covered faceted surfaces undergo further transformations upon annealing to temperatures ~1000 K; the surface is partially converted back to a planar one. This is evidenced by LEED patterns and by Pt and Ir $4f$ SXPS peak shapes. For the Pt/W system STM images of partially faceted and partially planar surfaces have been also published.[14] This phenomenon is likely to be associated with the decreasing amount of the overlayer material at the surface. Since the loss of facets occurs below the desorption threshold of Pt or Ir from W, the reason behind this could be the diffusion of Pt (or Ir) into the bulk driven by the entropy factor in the free energy. It may be deduced from binary-alloy phase diagrams[25,26] that each of the metals studied in this work has low solubility in a tungsten matrix, however, the solubility of Pt and Ir is significantly higher than that of Pd.

B. Multilayer films on W(111)

Previous studies of multilayer Pt film growth on W(111) by AES and LEED (Ref. 14) indicated that the growth is pseudomorphic, but not in a perfect layer-by-layer mode. In the present experiment this is confirmed for all four admetals studied since the attenuation of the substrate feature during growth is exponential and the LEED pattern remains (1×1) during growth but its sharpness deteriorates with increasing coverage. We conclude that the overlayers studied fully cover the substrate although their surfaces are not atomically flat. The growth proceeds in a random mode (similar to a ''sticks-where-it-hits'' mode). The $4f$ SXPS features (Pt and Ir) originating from multilayer films include the bulk feature and several components associated with different geometrical monolayers at the surface and at the interface. These multiple components appear at slightly different positions; their superposition forms a smooth curve which cannot be decomposed uniquely.

An interesting property of Pt, Rh, and Ir on W(111) is the mixing at the interface observed during deposition of overlayers at room temperature. Although the Pd/W system is chemically similar to the other systems studied, interface mixing does not occur for this case. In no case does the intermixing occur when the coverage is less than 1 ML. At 2–3-ML coverage the ''intermixed'' W peak is already clearly visible. The position of the peak corresponds to dilute W in a Pt (Ir, Rh) host. As indicated by the intensity of the ''intermixed'' peak, relative to the substrate peak, the mixing stops at 6–7-ML coverage. A very interesting aspect of this observation is that the adsorption of a metal atom at the film surface can trigger the site exchange process at a remote interface.

Recently Sprague and Gilmore[27] have shown by molecular-dynamics simulations that inelastic processess initiated by an atom impact on the surface can lead to interface mixing. In particular for Pt deposited on a Cu substrate a mixing has been found for thermal Pt energies. Interface mixing caused by electronic excitation has been reported also for a NiTi interface bombarded by GeV heavy ions.[28] It has been concluded that the mixing is caused by a short-lived lattice excitation in the immediate vicinity of an atom impact. The W/Pt (Ir, Rh) interface mixing observed in the course of our experiments can be described by similar words, although the exact nature of the phenomenon is not yet clear. The energetic barriers for intermixing are similar at all four interfaces studied (as indicated by similar thermal thresholds for mixing ~600 K, see the discussion below). The process is clearly driven by a release of energy upon adsorption of a metal atom on the film surface. Cohesive energies of metals studied have been compared in Table I. The energy for Pd is considerably smaller than for other metals and the presence of intermixing may be correlated with the value of the cohesive energy.

TABLE I. Relationship between cohesive energies and interface mixing during deposition of overlayers on a W substrate at 300 K.

Metal	Cohesive energy (eV/atom)	Mixing
Ir	6.95	yes
Pt	5.85	yes
Rh	5.76	yes
Pd	3.9	no

An interface between two metals formed at room temperature is typically metastable since interface diffusion barriers hinder intermixing. However, the mixing is likely to occur during annealing. In general there are several possibilities: e.g., for an A/B interface, A and B may preferentially remain in separate phases, or they may mix mutually, or A preferentially diffuses into B, or vice versa. In particular, if the deposited metal diffuses (dissolves) in the substrate, an ultrathin film of such a metal would, upon annealing, disappear from the surface, forming a dilute alloy with the substrate. However, if the deposited metal is not allowed to diffuse into the substrate it may stay on the surface as is, or form clusters, a surface alloy, or alloy clusters. Relevant examples, as seen by SXPS, have been demonstrated in our previous paper[4] for Pt, Pd, Ir, Rh, and Au on W(211). Films of Pt, Pd, Ir, or Rh on W(211) are transformed into flat alloy films upon annealing; a dilute alloy phase is observed below 900 K for Pt and Pd and below 1400 K for Ir and Rh. For higher annealing temperatures ($T>1400$ K) saturated alloy films are formed. Following SXPS peak assignments from Ref. 4 we are able to analyze the thermal evolution for more complex W(111)-based bimetallic systems. Ir on W(111) resembles closely Ir/W(211); initially a dilute W in the Ir alloy film is formed (600–1000 K). Above 1200 K a film of a saturated Ir-W alloy covers the W substrate.

Phenomena induced by heating Pt, Pd, and Rh films on W(111) are more diverse. Pt on W(111) resembles Pt on W(211) only during the dilute alloy phase at 600–900 K. In the case of Pd on W substantial corrugation of the film occurs before a dilute alloy is formed. For Rh films dilute alloy formation and initial film corrugation occur simultaneously. Since W atoms preferentially diffuse into Pt, Pd, and Rh the alloying process continues after formation of clusters. A common feature resulting from strong segregation trends (see Sec. IV A) is observed for all systems studied; a monolayer of late-transition metal always covers the tungsten substrate between clusters. Despite their chemical similarity, Ir, Pt, Pd, and Rh multilayer films exhibit different detailed behavior during annealing. The complexity in the electronic structure of transition-bimetallic systems means that the detailed structure and thermal transformations of a particular system cannot be predicted in a simple way. As discussed in Ref. 4 the observed SXPS peak shifts have no transparent relationship to alloy chemistry since the photoelectron peak shifts for transition metals are influenced by several competing effects; initial-state charge transfer tends to be rather small as the localized d orbital charge transfer is compensated for by a free s-, p-like charge. Other effects include final-state screening changes, intra-atomic shifts in valence level populations (rehybridization), or reference level changes.[29] The interplay of these many subtle effects is also impossible to predict in a simple way. Despite these difficulties, based on relative intensities of SXPS peaks, their order of appearance during growth, and their annealing behavior, it is possible to identify the chemical configuration of atoms emitting photoelectrons in particular SXPS lines and to successfully investigate the structure and transformations of the bimetallic system.

V. CONCLUSIONS

Several late-transition metals (Pt, Pd, Ir, Rh) grow in layers on W(111). The films have pseudomorphic structure for the initial few monolayers. A single monolayer of these metals on W(111) remains on the surface upon annealing, which is attributed to strong segregation trends of late-transition metals on W surfaces. The W(111) substrate covered with a single-monolayer film of a late-transition metal (Pt, Pd, Ir, Rh) and annealed is faceted to W(211). During growth of multilayer films of Pt, Ir, and Rh at room temperature, adsorption processess at the surface lead to mixing at the remote interface. Upon annealing, multilayer films of Pt, Pd, Ir, and Rh undergo complex transformations including alloying, segregation, clustering, and faceting of the surface between clusters. Although there are common features observed in the thermal evolution of these bimetallic systems, the detailed transformations are system-specific.

ACKNOWLEDGMENTS

This work has been supported in part by the U.S. Department of Energy, Office of Basic Energy Sciences and by the U.S. Army Research Office.

*Present address: Instytut Fizyki, Uniwersytet Jagiellonski, Reymonta 4, 30-059 Krakow, Poland.

†Corresponding author.

[1] T.E. Madey, J. Guan, C.-H. Nien, C.-Z. Dong, H.-S. Tao, and R.A. Campbell, Surf. Rev. Lett. **3**, 1315 (1996).

[2] T.E. Madey, C.-H. Nien, K. Pelhos, J.J. Kolodziej, I.M. Abdelrehim, and H.-S. Tao, Surf. Sci. **438**, 191 (1999).

[3] J.J. Kolodziej, K. Pelhos, I.M. Abdelrehim, J.W. Keister, J.E. Rowe, and T.E. Madey, Prog. Surf. Sci. **59**, 117 (1999).

[4] J.J. Kolodziej, T.E. Madey, J.W. Keister, and J.E. Rowe, Phys. Rev. B **62**, 5150 (2000).

[5] G.A. Attard and D.A. King, Surf. Sci. **222**, 360 (1989).

[6] R.W. Judd, M.A. Reichelt, E.G. Scott, and R.M. Lambert, Surf. Sci. **185**, 515 (1987).

[7] A. Christensen, A.V. Ruban, P. Stoltze, K.W. Jacobsen, H.L. Skriver, and J.K. Norskov, Phys. Rev. B **56**, 5822 (1997).

[8] J.G. Che, C.T. Chan, C.H. Kuo, and T.C. Leung, Phys. Rev. Lett. **79**, 4230 (1997).

[9] A.M.N. Niklasson, I.A. Abrikosov, and B. Johansson, Phys. Rev. B **58**, 3613 (1998).

[10] D. Wu, W.K. Lau, Z.Q. He, Y.J. Feng, M.S. Altman, and C.T. Chan, Phys. Rev. B **62**, 8366 (2000).

[11] A.V. Ruban, H.L. Skriver, and J.K. Norskov, Phys. Rev. B **59**, 15 990 (1999).
[12] P. Thiry, P.A. Bennett, S.D. Kevan, W.A. Royer, E.E. Chaban, J.E. Rowe, and N.V. Smith, Nucl. Instrum. Methods Phys. Res. A **222**, 85 (1984).
[13] W. Xu and J.B. Adams, Surf. Sci. **319**, 45 (1994).
[14] C.Z. Dong, S.M. Shivaprasad, K.-J. Song, and T.E. Madey, J. Chem. Phys. **99**, 9172 (1993).
[15] K.-J Song, C.-Z Dong, and T.E. Madey, Langmuir **7**, 3019 (1991).
[16] H.-S Tao, J.E. Rowe, and T.E. Madey, Surf. Sci. **407**, L640 (1998).
[17] H.-S Tao, C.-H. Nien, T.E. Madey, J.E. Rowe, and G.K. Wertheim, Surf. Sci. **357**, 55 (1996).
[18] K. Pelhos, Ph.D. thesis, Rutgers University, 1999.
[19] I.A. Abrikosov, A.V. Ruban, H.L. Skriver, and B. Johansson, Phys. Rev. B **50**, 2039 (1994).
[20] A.V. Ruban and H.L. Skriver, Comput. Mater. Sci. **15**, 119 (1999).
[21] C.Z. Dong, L. Zhang, U. Diebold, and T.E. Madey, Surf. Sci. **322**, 221 (1995).
[22] J.G. Che, C.T. Chan, C.H. Kuo, and T.C. Leung, Phys. Rev. Lett. **79**, 4230 (1997).
[23] K. Pelhos, J.B. Hannon, G.L. Kellogg, and T.E. Madey, Surf. Sci. **432**, 115 (1999).
[24] K. Pelhos, T.E. Madey, J.B. Hannon, and G.L. Kellogg, Surf. Rev. Lett. **5**, 767 (1999).
[25] F.A. Shunk and M. Hansen, *Constitution of Binary Alloys, 2nd Supplement* (McGraw-Hill, New York, 1969).
[26] R.P. Elliot and M. Hansen, *Constitution of Binary Alloys, 1st Supplement*, (McGraw-Hill, New York, 1965).
[27] J.A. Sprague and C.M. Gilmore, Thin Solid Films **272**, 244 (1996).
[28] R. Leguay, A. Dunlop, F. Dunstetter, N. Lorenzelli, A. Braslau, F. Bridou, J. Corno, B. Pardo, J. Chevallier, C. Colliex, A. Menelle, J.L. Rouviere, and L. Thome, Nucl. Instrum. Methods Phys. Res. B **122**, 481 (1997).
[29] R.E. Watson and M.L. Perlman, Phys. Scr. **21**, 527 (1980).